ACS Partner Journal
PRECISION CHEMISTRY

pubs.acs.org/PrecisionChem
Article

Thiol Ligand-Modified Au for Highly Efficient Electroreduction of Nitrate to Ammonia

Yuheng Wu, Xiangdong Kong, Yechao Su, Jiankang Zhao, Yiling Ma, Tongzheng Ji, Di Wu, Junyang Meng, Yan Liu,* Zhigang Geng,* and Jie Zeng*

Cite This: *Precis. Chem.* 2024, 2, 112−119
Read Online

ACCESS | Metrics & More | Article Recommendations | Supporting Information

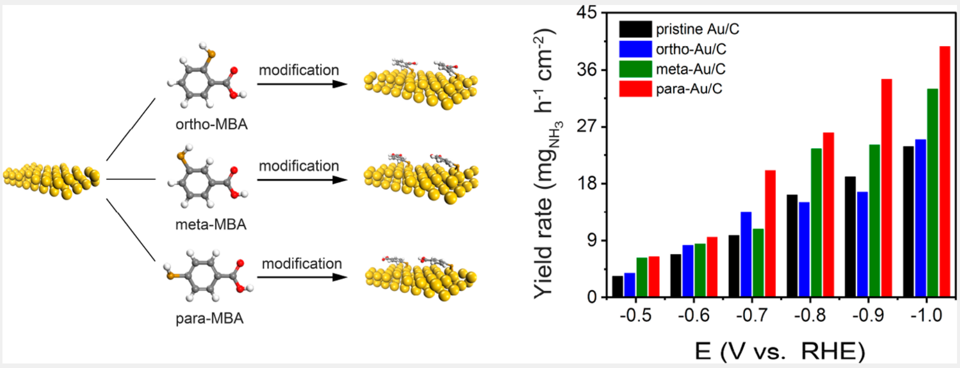

ABSTRACT: Electroreduction of nitrate (NO_3^-) to ammonia (NH_3) is an environmentally friendly route for NH_3 production, serving as an appealing alternative to the Haber−Bosch process. Recently, various noble metal-based electrocatalysts have been reported for electroreduction of NO_3^-. However, the application of pure metal electrocatalysts is still limited by unsatisfactory performance, owing to the weak adsorption of nitrogen-containing intermediates on the surface of pure metal electrocatalysts. In this work, we report thiol ligand-modified Au nanoparticles as the effective electrocatalysts toward electroreduction of NO_3^-. Specifically, three mercaptobenzoic acid (MBA) isomers, thiosalicylic acid (ortho-MBA), 3-mercaptobenzoic acid (meta-MBA), and 4-mercaptobenzoic acid (para-MBA), were employed to modify the surface of the Au nanocatalyst. During the NO_3^- electroreduction, para-MBA modified Au (denoted as para-Au/C) displayed the highest catalytic activity among these Au-based catalysts. At −1.0 V versus reversible hydrogen electrode (vs RHE), para-Au/C exhibited a partial current density for NH_3 of 472.2 mA cm^{-2}, which was 1.7 times that of the pristine Au catalyst. Meanwhile, the Faradaic efficiency (FE) for NH_3 reached 98.7% at −1.0 V vs RHE for para-Au/C. The modification of para-MBA significantly improved the intrinsic activity of the Au/C catalyst, thus accelerating the kinetics of NO_3^- reduction and giving rise to a high NH_3 yield rate of para-Au/C.

KEYWORDS: *Ammonia synthesis, NO_3^- electroreduction, Au nanoparticles, thiol ligand modification, electronic structure*

■ INTRODUCTION

As one of the most fundamental industrial products, ammonia (NH_3) is not only an indispensable chemical in fertilizer, medicine, dye, and other industries but also an important carbon-free energy storage medium.[1−3] Currently, the predominant method of NH_3 synthesis, the Haber−Bosch process, requires extreme reaction conditions of high temperature (400−500 °C) and high pressure (150−300 bar) with only 10−20% conversion efficiency.[4−6] It is reported that the annual energy consumption for NH_3 synthesis accounts for 1−2% of the total global energy supply accompanied by about 1.5% of the global carbon emissions, leading to significant damage to the natural environment.[7−11] Therefore, a clean and economical route for NH_3 production is urgently needed in pursuit of a sustainable chemical industry.[12−15]

Over the past few decades, the electroreduction of nitrate (NO_3^-) to NH_3 stands out as one of the desirable pathways for NH_3 production as an alternative to the Haber−Bosch process.[16−20] Besides, nitrate pollution in water has long been a serious environmental issue all over the world. The high concentration of nitrate in the water body is one of the main reasons for aquatic ecosystem damage and the increase of certain human diseases.[20−22] Utilizing NO_3^- as the nitrogen source for NH_3 synthesis not only satisfies the tremendous

Received: November 9, 2023
Revised: January 25, 2024
Accepted: January 25, 2024
Published: February 15, 2024

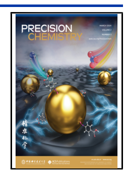

https://doi.org/10.1021/prechem.3c00107
Precis. Chem. 2024, 2, 112−119

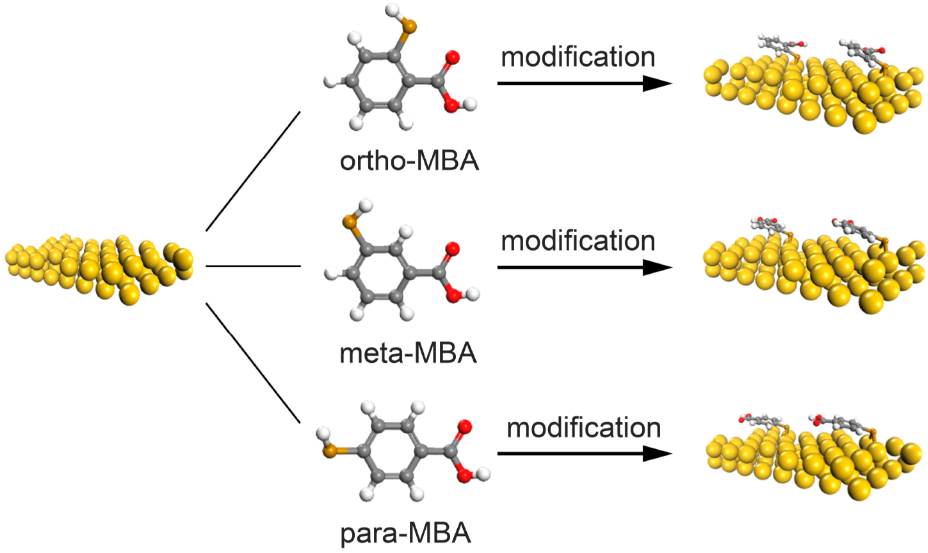

Figure 1. Schematic illustration of the synthesis of thiol ligand-modified Au/C. The gold, gray, red, brown, and white spheres represent Au, C, O, S, and H atoms, respectively.

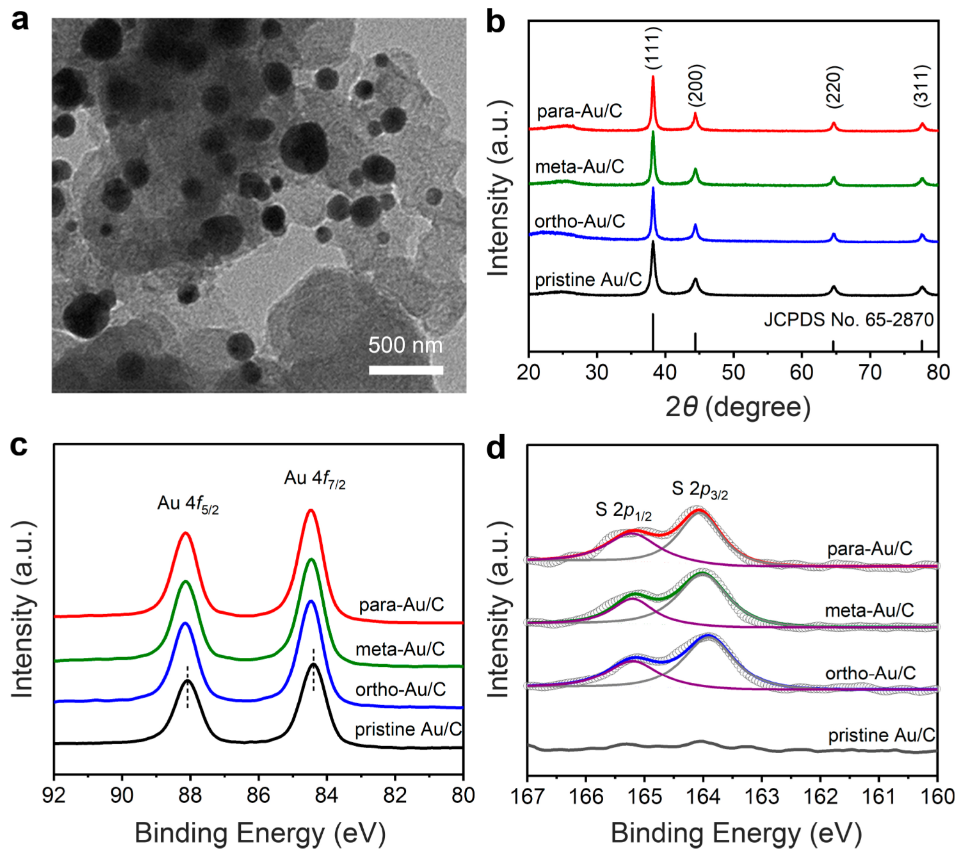

Figure 2. (a) TEM image of para-Au/C. (b) XRD, (c) Au 4*f* XPS, and (d) S 2*p* XPS of pristine Au/C, ortho-Au/C, meta-Au/C, and para-Au/C.

demand of NH_3 but also helps mediate the disrupted nitrogen cycle.[3,22] Recently, various metal-based electrocatalysts such as Ir,[23] Pd,[24] Ru,[25] Ag,[26] and Au[27] have been reported for NO_3^- electroreduction. However, the application of pure metal electrocatalysts is still limited by unsatisfactory performance owing to the weak adsorption of nitrogen-containing intermediates on the surface of pure metal electrocatalysts.[28,29] Thus, developing an effective method of modulating the electronic structure is crucial to enhancing the intrinsic activity of pristine catalysts. Among various strategies to manipulate the electronic structures of electrocatalysts, ligand modification is considered especially appealing due to its simplicity and effectiveness in tuning the electronic properties of the catalytic active sites.[30,31] For instance, the ligand X (X = O, OH, F, Cl, Br, and I) axially ligated to Fe–N_4 notably improved the kinetics of the rate-determining step in NO_3^- reduction, owing to the change of the *d*-band center spin state gap of Fe^{3d}.[32] Besides, pyridine functionalization can remarkably augment

https://doi.org/10.1021/prechem.3c00107
Precis. Chem. 2024, 2, 112–119

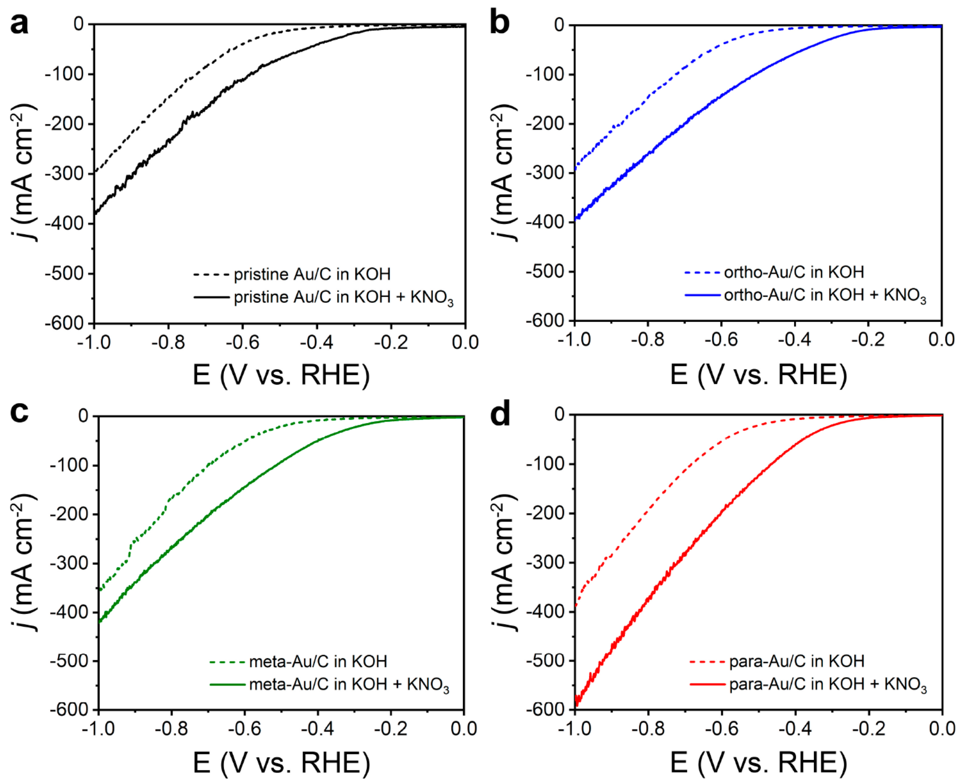

Figure 3. LSV of (a) pristine Au/C, (b) ortho-Au/C, (c) meta-Au/C, and (d) para-Au/C in 1.0 M KOH with/without 0.1 M KNO_3 electrolyte.

the activity of Ag nanosheet toward NO_3^- reduction due to the promoted adsorption of NO_3^-.[28] As such, it is highly desirable to explore the ligand effect on metal-based catalysts toward the electroreduction of NO_3^- through the modification of thiol ligands.

In this work, we report a thiol ligand modification method to enhance the performance of Au nanoparticles for the electroreduction of NO_3^- to NH_3. We employed three mercaptobenzoic acid (MBA) isomers, including thiosalicylic acid (ortho-MBA), 3-mercaptobenzoic acid (meta-MBA), and 4-mercaptobenzoic acid (para-MBA), to modify Au nanoparticles (Figure 1). Para-MBA modified Au catalyst (denoted as para-Au/C) exhibited the best performance among these Au-based catalysts. The partial current density for NH_3 (j_{NH_3}) of para-Au/C reached 472.2 mA cm^{-2} with a Faradaic efficiency (FE) up to 98.7% at the potential of −1.0 V versus reversible hydrogen electrode (vs RHE). Besides, the highest yield rate of NH_3 for para-Au/C was 39.7 mg h^{-1} cm^{-2} at −1.0 V vs RHE, which was 1.7 times that of pristine Au catalyst (denoted as pristine Au/C). The modification of para-MBA significantly improved the intrinsic activity of the Au/C catalyst, thus accelerating the kinetics of NO_3^- reduction and giving rise to a high NH_3 yield rate of para-Au/C.

■ RESULTS AND DISCUSSION

Synthesis and Characterizations of Thiol-Modified Au Nanoparticles

The Au nanoparticles were fabricated by chemical reduction of $HAuCl_4$ using $NaBH_4$, followed by immobilization on carbon black and soaking in MBA solutions.[33] Au nanoparticles modified by ortho-MBA, meta-MBA, and para-MBA were denoted as ortho-Au/C, meta-Au/C, and para-Au/C, respectively. For comparison, a pristine Au/C catalyst was prepared in the same process without the soaking step. The transmission electron microscopy (TEM) image of pristine Au/C catalyst clearly depicted the spherical morphology of Au nanoparticles, which were uniformly dispersed on carbon black (Figure S1). After the thiol ligand modification, the morphology and size distribution of ortho-Au/C, meta-Au/C, and para-Au/C displayed no obvious change (Figures 2a, S2, and S3). The X-ray diffraction (XRD) patterns of the catalysts revealed that the metallic Au exhibited a face-centered cubic (fcc) crystal structure with distinct diffraction peaks at 38.2°, 44.4°, 64.6°, and 77.6°, corresponding to the (111), (200), (220), and (311) facets, respectively (Figure 2b).[33] In this case, the phase structure of the Au nanoparticles did not alter significantly after the ligand modification. The high resolution transmission electron microscopy (HRTEM) image of para-Au/C delivered interplanar spacings of 2.36, 2.03, and 1.44 Å, which corresponded to the (111), (200), and (220) facets of Au, respectively (Figure S4a). The selected area electron diffraction (SAED) pattern of para-Au/C exhibited circular rings corresponding to (111), (200), and (222) facets of Au, revealing its polycrystalline nature (Figure S4b). The result of energy-dispersive X-ray spectroscopy (EDS) mapping displayed the uniform distribution of the S element around Au nanoparticles, indicating the accurate attachment of para-MBA to Au atoms in para-Au/C (Figure S5). The X-ray photoelectron spectroscopy (XPS) of Au 4*f* spectrum of pristine Au/C exhibited two distinct peaks at 84.4 and 88.1 eV, corresponding to $4f_{7/2}$ and $4f_{5/2}$ of metallic Au species, respectively (Figure 2c).[33] Notably, the Au $4f_{7/2}$ XPS peaks of modified Au/C shifted by ~0.05 eV to higher binding energy, which was derived from the electron interaction between Au and S.[34] Moreover, the S 2*p* XPS spectrum of pristine Au/C showed no signal of S (Figure 2d). In contrast, the modified Au/C revealed two peaks at around 164 and 165 eV,

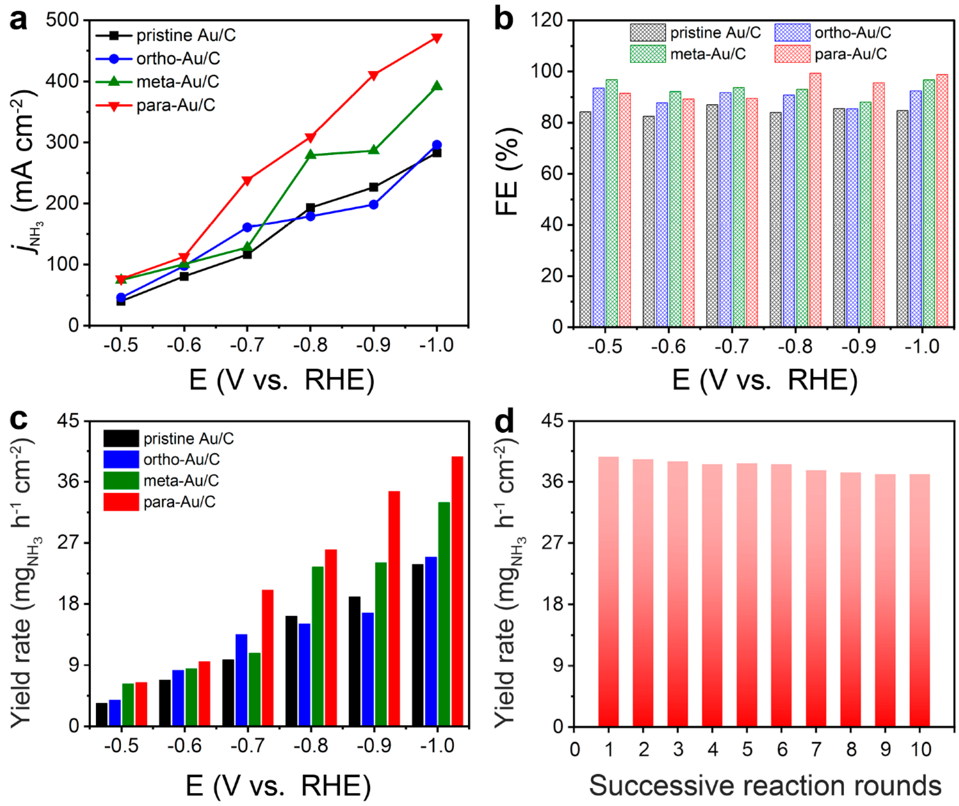

Figure 4. (a) j_{NH_3}, (b) FE, and (c) yield rate of NH_3 of pristine Au/C, ortho-Au/C, meta-Au/C, and para-Au/C at different applied potentials. (d) The cyclic electrolysis test of para-Au/C at −1.0 V vs RHE.

respectively corresponding to S $2p_{3/2}$ and S $2p_{1/2}$ spectra.[36] Compared with the pristine thiol ligands, the shift of S $2p_{3/2}$ peaks for the modified Au/C catalysts followed the order of para-Au/C > meta-Au/C > ortho-Au/C (Figure S6). In this case, the interaction between Au and S for para-Au/C was the strongest among the modified Au/C catalysts, inducing the strongest regulation of the electronic structure of para-Au/C.

Catalytic Performance of NO_3^- Electroreduction

The electrochemical catalytic performance was measured under ambient conditions in a H-cell. The linear sweep voltammetry (LSV) experiments of Au/C catalysts were conducted in 1.0 M KOH electrolyte with and without 0.1 M KNO_3 (Figure 3). In LSV tests, all four Au/C catalysts delivered much larger current densities in 1.0 M KOH + 0.1 M KNO_3 electrolyte than those in 1.0 M KOH alone at the same potential, suggesting that the kinetics of NO_3^- electroreduction was much faster than that of H_2 evolution.[35] Besides, the modified Au/C catalysts yielded impressively higher current densities than pristine Au/C, meaning that thiol ligand modification significantly enhanced the catalytic activity of the Au/C catalyst. Among the four catalysts, para-Au/C delivered the highest current density in 1.0 M KOH + 0.1 M KNO_3 electrolyte, implying its highest activity toward NO_3^- electroreduction. Notably, compared with pristine Au/C, the increment of current densities for para-Au/C in the KOH electrolyte with KNO_3 was considerably greater than those in KOH alone, meaning that the ligand effect had a more pronounced influence on electroreduction of NO_3^- compared with its impact on H_2 evolution.

To evaluate the catalytic performance of each Au/C catalyst, we conducted electrolysis experiments at different applied potentials for 1 h. The concentration of NH_3 was determined using the indophenol blue method by UV−vis (Figure S7). Figure 4a illustrates the partial current densities for NH_3 (j_{NH_3}) on four Au/C catalysts. Compared with pristine Au/C, all of the modified Au/C catalysts demonstrated a substantial increment of j_{NH_3}. Among these modified catalysts, para-Au/C displayed the highest j_{NH_3}, reaching 472.2 mA cm^{-2} at the potential of −1.0 V vs RHE. Figure 4b shows the FE for NH_3 of Au/C catalysts during electrolysis. Compared with pristine Au/C, all of the modified catalysts exhibited increased FE for NH_3 production. Especially, para-Au/C displayed a maximal FE of 99.3% at −0.8 V vs RHE. Figure 4c depicts the NH_3 yield rates of Au/C catalysts at different applied potentials. Remarkably, para-Au/C exhibited the highest NH_3 yield rate among the three modified catalysts, reaching 39.7 mg h^{-1} cm^{-2} at −1.0 V vs RHE. Moreover, the para-Au/C catalyst outperformed most of the reported Au-based electrocatalysts, demonstrating the effectivity of thiol modification as a simple strategy for boosting the catalytic performance (Table S1). Besides, the investigation into the effect of Au loading and soaking time on catalytic performance demonstrated that the optimized Au loading and soaking time were 25 wt % and 1 h, respectively (Figures S8 and S9). The stability test for para-Au/C catalyst was conducted in 1.0 M KOH + 0.1 M KNO_3 electrolyte at −1.0 V vs RHE (Figure 4d). In 10 successive reaction rounds, para-Au/C showed negligible performance degradation, exhibiting only a 6.5% decay for the yield rate of NH_3. The TEM image and XRD pattern of para-Au/C after cyclic electrolysis displayed no obvious change, representing the structural robustness of para-Au/C (Figure S10). In addition, a ^{15}N isotope-labeling experiment was conducted to

https://doi.org/10.1021/prechem.3c00107
Precis. Chem. 2024, 2, 112−119

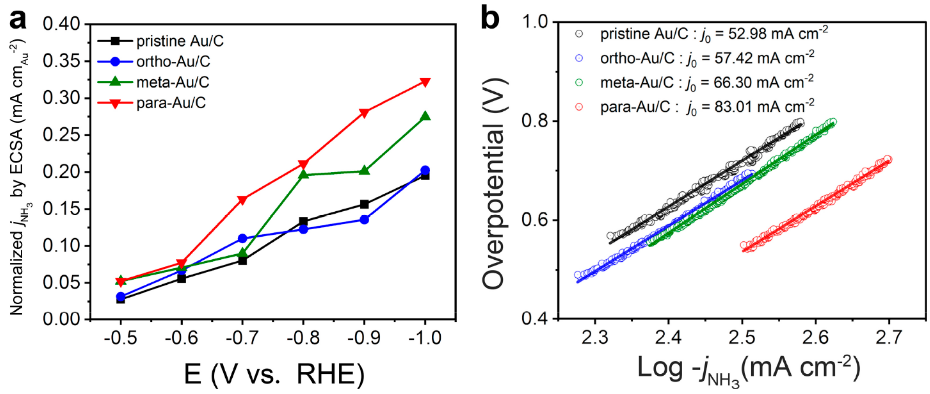

Figure 5. (a) ECSA normalized partial current densities for NH_3. (b) Tafel plot of pristine Au/C, ortho-Au/C, meta-Au/C, and para-Au/C in 1.0 M KOH with 0.1 M KNO_3 electrolyte. The j_0 was derived from the intercept of the linear region in Tafel plots.

further quantify the product (Figure S11). The FE for NH_3 at −0.6 V vs RHE determined by ^{1}H NMR was approximated to the results detected via the UV−vis method (Figure S12). These results verified that the generated NH_3 originated from the electroreduction of NO_3^-.

To clarify the intrinsic activity of modified Au/C, the double-layer capacitance (C_{dl}) was measured to calculate the electrochemical active surface areas (ECSAs) of Au/C catalysts.[36] Cyclic voltammetry (CV) of Au/C catalysts was measured at different scan rates, ranging from 20 to 100 mV s^{-1} (Figure S13). The charging current densities at each scan rate were used to determine the C_{dl} of the working electrodes (Figure S14).[37] The C_{dl} of pristine Au/C, ortho-Au/C, meta-Au/C, and para-Au/C was calculated to be 11.6, 11.7, 11.4, and 11.7 mF cm^{-2}, respectively, meaning that the four catalysts had similar ECSAs. Then we normalized the j_{NH_3} based on ECSA.[38] As shown in Figure 5a, para-Au/C delivered the highest normalized j_{NH_3} among the four Au/C catalysts, indicating that the modification of para-MBA to Au nanoparticles significantly improved the intrinsic activity. Figure S15 displays the electrochemical impedance spectroscopy (EIS) of Au/C catalysts. As shown in the high frequency region of the Nyquist plot, para-Au/C had the lowest charge transfer resistance (R_{ct}) among these Au/C catalysts, suggesting that the charge transfer on para-Au/C was the fastest.[39] To evaluate the kinetics of NO_3^- reduction, we calculated the exchange current densities (j_0) of each Au/C catalyst based on Tafel plots (Figure 5b). Obviously, the values of j_0 followed the order of para-Au/C > meta-Au/C > ortho-Au/C > pristine Au/C. According to the Butler−Volmer equation, the largest j_0 of para-Au/C represented the fastest kinetics of NO_3^- reduction among all four catalysts, thus giving rise to its highest catalytic activity.[40−42] To further elucidate the effect of the ligand on Au/C, density functional theory (DFT) calculations were performed to evaluate the adsorption of NO_3^- on pristine Au (111) and para-MBA modified Au (111) (donated as pristine Au and para-Au), respectively (Figure S16). Compared with pristine Au, para-Au exhibited a lower ΔG_{ads} for NO_3^-, indicating that para-Au possessed stronger binding with NO_3^-. In this case, the boosted catalytic performance of para-Au could be attributed to the facilitated adsorption of NO_3^- on the surface of para-Au.

■ CONCLUSION

In this work, we developed a simple method of thiol ligand modification to promote the catalytic performance of Au catalyst toward electroreduction of NO_3^- to NH_3. Among all the modified Au/C catalysts, para-Au/C achieved the j_{NH_3} of 472.2 mA cm^{-2} with the FE up to 98.7% at the potential of −1.0 V vs RHE. Remarkably, the highest yield rate of NH_3 for para-Au/C reached up to 39.7 mg h^{-1} cm^{-2} at −1.0 V vs RHE, which was 1.7 times that of pristine Au/C. Para-MBA modification significantly improved the intrinsic activity of Au/C catalyst, thus accelerating the kinetics of NO_3^- reduction and giving rise to the high NH_3 yield rate of para-Au/C. This work offers an effective chemical modification strategy for guiding the rational design of noble-metal-based electrocatalysts toward NO_3^- reduction.

■ ASSOCIATED CONTENT

Supporting Information

The Supporting Information is available free of charge at https://pubs.acs.org/doi/10.1021/prechem.3c00107.

Experimental and computational methods; TEM image and size distribution of Au nanoparticles for pristine Au/C, ortho-Au/C, meta-Au/C, and para-Au/C; HRTEM image and EDS mapping of para Au/C; S 2*p* XPS spectra of ortho-MBA, meta-MBA, and para-MBA; determination of NH_3 and $^{15}NH_3$; catalytic performance of para-Au/C with different Au loading and soaking time; CV curves, C_{dl}, Nyquist plots for pristine Au/C, ortho-Au/C, meta-Au/C, and para-Au/C; DFT calculation of adsorption for $*NO_3$ on pristine Au and para-Au (PDF)

■ AUTHOR INFORMATION

Corresponding Authors

Yan Liu − *Hefei National Research Center for Physical Sciences at the Microscale, Key Laboratory of Strongly-Coupled Quantum Matter Physics of Chinese Academy of Sciences, Key Laboratory of Surface and Interface Chemistry and Energy Catalysis of Anhui Higher Education Institutes, Department of Chemical Physics, University of Science and Technology of China, Hefei, Anhui 230026, P. R. China*; Email: yliu1993@ustc.edu.cn

Zhigang Geng − *Hefei National Research Center for Physical Sciences at the Microscale, Key Laboratory of Strongly-*

Coupled Quantum Matter Physics of Chinese Academy of Sciences, Key Laboratory of Surface and Interface Chemistry and Energy Catalysis of Anhui Higher Education Institutes, Department of Chemical Physics, University of Science and Technology of China, Hefei, Anhui 230026, P. R. China; orcid.org/0000-0003-3183-5900; Email: gengzg@ustc.edu.cn

Jie Zeng – *Hefei National Research Center for Physical Sciences at the Microscale, Key Laboratory of Strongly-Coupled Quantum Matter Physics of Chinese Academy of Sciences, Key Laboratory of Surface and Interface Chemistry and Energy Catalysis of Anhui Higher Education Institutes, Department of Chemical Physics, University of Science and Technology of China, Hefei, Anhui 230026, P. R. China; School of Chemistry & Chemical Engineering, Anhui University of Technology, Ma'anshan, Anhui 243002, P. R. China;* orcid.org/0000-0002-8812-0298; Email: zengj@ustc.edu.cn

Authors

Yuheng Wu – *Hefei National Research Center for Physical Sciences at the Microscale, Key Laboratory of Strongly-Coupled Quantum Matter Physics of Chinese Academy of Sciences, Key Laboratory of Surface and Interface Chemistry and Energy Catalysis of Anhui Higher Education Institutes, Department of Chemical Physics, University of Science and Technology of China, Hefei, Anhui 230026, P. R. China*

Xiangdong Kong – *Hefei National Research Center for Physical Sciences at the Microscale, Key Laboratory of Strongly-Coupled Quantum Matter Physics of Chinese Academy of Sciences, Key Laboratory of Surface and Interface Chemistry and Energy Catalysis of Anhui Higher Education Institutes, Department of Chemical Physics, University of Science and Technology of China, Hefei, Anhui 230026, P. R. China*

Yechao Su – *Hefei National Research Center for Physical Sciences at the Microscale, Key Laboratory of Strongly-Coupled Quantum Matter Physics of Chinese Academy of Sciences, Key Laboratory of Surface and Interface Chemistry and Energy Catalysis of Anhui Higher Education Institutes, Department of Chemical Physics, University of Science and Technology of China, Hefei, Anhui 230026, P. R. China*

Jiankang Zhao – *Hefei National Research Center for Physical Sciences at the Microscale, Key Laboratory of Strongly-Coupled Quantum Matter Physics of Chinese Academy of Sciences, Key Laboratory of Surface and Interface Chemistry and Energy Catalysis of Anhui Higher Education Institutes, Department of Chemical Physics, University of Science and Technology of China, Hefei, Anhui 230026, P. R. China*

Yiling Ma – *Hefei National Research Center for Physical Sciences at the Microscale, Key Laboratory of Strongly-Coupled Quantum Matter Physics of Chinese Academy of Sciences, Key Laboratory of Surface and Interface Chemistry and Energy Catalysis of Anhui Higher Education Institutes, Department of Chemical Physics, University of Science and Technology of China, Hefei, Anhui 230026, P. R. China*

Tongzheng Ji – *Hefei National Research Center for Physical Sciences at the Microscale, Key Laboratory of Strongly-Coupled Quantum Matter Physics of Chinese Academy of Sciences, Key Laboratory of Surface and Interface Chemistry and Energy Catalysis of Anhui Higher Education Institutes, Department of Chemical Physics, University of Science and Technology of China, Hefei, Anhui 230026, P. R. China*

Di Wu – *Hefei National Research Center for Physical Sciences at the Microscale, Key Laboratory of Strongly-Coupled Quantum Matter Physics of Chinese Academy of Sciences, Key Laboratory of Surface and Interface Chemistry and Energy Catalysis of Anhui Higher Education Institutes, Department of Chemical Physics, University of Science and Technology of China, Hefei, Anhui 230026, P. R. China*

Junyang Meng – *Hefei National Research Center for Physical Sciences at the Microscale, Key Laboratory of Strongly-Coupled Quantum Matter Physics of Chinese Academy of Sciences, Key Laboratory of Surface and Interface Chemistry and Energy Catalysis of Anhui Higher Education Institutes, Department of Chemical Physics, University of Science and Technology of China, Hefei, Anhui 230026, P. R. China*

Complete contact information is available at:
https://pubs.acs.org/10.1021/prechem.3c00107

Notes

The authors declare no competing financial interest.

■ ACKNOWLEDGMENTS

This work was supported by Strategic Priority Research Program of the Chinese Academy of Sciences (XDB0450401), National Key Research and Development Program of China (2021YFA1500500 and 2019YFA0405600), NSFC (22209161, 22209163, 92061111, 22322901, 22221003, and 22250007), CAS Project for Young Scientists in Basic Research (YSBR-051 and YSBR-022), National Science Fund for Distinguished Young Scholars (21925204), China Post-doctoral Program for Innovative Talents (BX20200324), and Fundamental Research Funds for the Central Universities. J.Z. acknowledges support from the Tencent Foundation through the XPLORER PRIZE. The authors acknowledge support from Prof. Chao Ma and Mr. Sunpei Hu in conducting the microscopic characterization, and Dr. Hong Wu in the DFT computations. This work was partially carried out at the Instruments Center for Physical Science, University of Science and Technology of China. This work was also partially carried out at the USTC Center for Micro and Nanoscale Research and Fabrication.

■ REFERENCES

(1) Chen, J. G.; Crooks, R. M.; Seefeldt, L. C.; Bren, K. L.; Bullock, R. M.; Darensbourg, M. Y.; Holland, P. L.; Hoffman, B.; Janik, M. J.; Jones, A. K.; et al. Beyond fossil fuel-driven nitrogen transformations. *Science* **2018**, *360*, 6391.

(2) Suryanto, B. H.; Du, H. L.; Wang, D.; Chen, J.; Simonov, A. N.; MacFarlane, D. R. Challenges and prospects in the catalysis of electroreduction of nitrogen to ammonia. *Nat. Catal.* **2019**, *2*, 290–296.

(3) Chen, F. Y.; Wu, Z. Y.; Gupta, S.; Rivera, D. J.; Lambeets, S. V.; Pecaut, S.; Kim, J. Y. T.; Zhu, P.; Finfrock, Y. Z.; Meira, D. M.; et al. Efficient conversion of low-concentration nitrate sources into ammonia on a Ru-dispersed Cu nanowire electrocatalyst. *Nat. Nanotechnol.* **2022**, *17*, 759–767.

(4) Inoue, Y.; Kitano, M.; Kishida, K.; Abe, H.; Niwa, Y.; Sasase, M.; Fujita, Y.; Ishikawa, H.; Yokoyama, T.; Hara, M.; Hosono, H. Efficient and stable ammonia synthesis by self-organized flat Ru nanoparticles on calcium amide. *ACS Catal.* **2016**, *6*, 7577–7584.

(5) Liu, S.; Wang, M.; Qian, T.; Ji, H.; Liu, J.; Yan, C. Facilitating nitrogen accessibility to boron-rich covalent organic frameworks via electrochemical excitation for efficient nitrogen fixation. *Nat. Commun.* **2019**, *10*, 3898.

(6) Song, Z.; Liu, Y.; Zhao, J.; Zhong, Y.; Qin, L.; Guo, Q.; Geng, Z.; Zeng, J. Promoting N_2 electroreduction into NH_3 over porous carbon by introducing oxygen-containing groups. *Chem. Eng. J.* **2022**, *434*, No. 134636.
(7) Van der Ham, C. J.; Koper, M. T.; Hetterscheid, D. G. Challenges in reduction of dinitrogen by proton and electron transfer. *Chem. Soc. Rev.* **2014**, *43*, 5183−5191.
(8) Qing, G.; Ghazfar, R.; Jackowski, S. T.; Habibzadeh, F.; Ashtiani, M. M.; Chen, C. P.; Smith, M. R., III; Hamann, T. W. Recent advances and challenges of electrocatalytic N_2 reduction to ammonia. *Chem. Rev.* **2020**, *120*, 5437−5516.
(9) Minteer, S. D.; Christopher, P.; Linic, S. Recent developments in nitrogen reduction catalysts: A virtual issue. *ACS Energy Lett.* **2019**, *4*, 163−166.
(10) Lazouski, N.; Steinberg, K. J.; Gala, M. L.; Krishnamurthy, D.; Viswanathan, V.; Manthiram, K. Proton donors induce a differential transport effect for selectivity toward ammonia in lithium-mediated nitrogen reduction. *ACS Catal.* **2022**, *12*, 5197−5208.
(11) Kandemir, T.; Schuster, M. E.; Senyshyn, A.; Behrens, M.; Schlögl, R. The Haber-Bosch Process Revisited: On the real structure and stability of "ammonia iron" under working condition. *Angew. Chem., Int. Ed.* **2013**, *52*, 12723−12726.
(12) Yu, M. S.; Jesudass, S. C.; Surendran, S.; Kim, J. Y.; Sim, U.; Han, M. K. Synergistic interaction of MoS_2 nanoflakes on $La_2Zr_2O_7$ nanofibers for improving photoelectrochemical nitrogen reduction. *ACS Appl. Mater. Interfaces* **2022**, *14*, 31889−31899.
(13) Kim, D.; Surendran, S.; Janani, G.; Lim, Y.; Choi, H.; Han, M. K.; Yuvaraj, S.; Kim, T. H.; Kim, J. K.; Sim, U. Nitrogen-impregnated carbon-coated TiO_2 nanoparticles for N_2 reduction to ammonia under ambient conditions. *Mater. Lett.* **2022**, *314*, No. 131808.
(14) Kim, D.; Surendran, S.; Lim, Y.; Choi, H.; Lim, J.; Kim, J. Y.; Han, M. K.; Sim, U. Spinel-type Ni_2GeO_4 electrocatalyst for electrochemical ammonia synthesis via nitrogen reduction reaction under ambient conditions. *Int. J. Energy Res.* **2022**, *46*, 4119−4129.
(15) Jeong, Y.; Janani, G.; Kim, D.; An, T. Y.; Surendran, S.; Lee, H.; Moon, D. J.; Kim, J. Y.; Han, M. K.; Sim, U. Roles of heterojunction and Cu vacancies in the Au@Cu_{2-x}Se for the enhancement of electrochemical nitrogen reduction performance. *ACS Appl. Mater. Interfaces* **2023**, *15*, 52342−52357.
(16) Chen, G. F.; Cao, X.; Wu, S.; Zeng, X.; Ding, L. X.; Zhu, M.; Wang, H. Ammonia electrosynthesis with high selectivity under ambient conditions via a Li^+ incorporation strategy. *J. Am. Chem. Soc.* **2017**, *139*, 9771−9774.
(17) Chen, G. F.; Yuan, Y.; Jiang, H.; Ren, S. Y.; Ding, L. X.; Ma, L.; Wu, T.; Lu, J.; Wang, H. Electrochemical reduction of nitrate to ammonia via direct eight-electron transfer using a copper-molecular solid catalyst. *Nat. Energy* **2020**, *5*, 605−613.
(18) Li, J.; Zhan, G.; Yang, J.; Quan, F.; Mao, C.; Liu, Y.; Wang, B.; Lei, F.; Li, L.; Chan, A. W.; Xu, L.; et al. Efficient ammonia electrosynthesis from nitrate on strained ruthenium nanoclusters. *J. Am. Chem. Soc.* **2020**, *142*, 7036−7046.
(19) Sun, W. J.; Ji, H. Q.; Li, L. X.; Zhang, H. Y.; Wang, Z. K.; He, J. H.; Lu, J. M. Built-in electric field triggered interfacial accumulation effect for efficient nitrate removal at ultra-low concentration and electroreduction to ammonia. *Angew. Chem., Int. Ed.* **2021**, *60*, 22933−22939.
(20) van Langevelde, P. H.; Katsounaros, I.; Koper, M. T. Electrocatalytic nitrate reduction for sustainable ammonia production. *Joule* **2021**, *5*, 290−294.
(21) Zhang, X.; Wang, Y.; Liu, C.; Yu, Y.; Lu, S.; Zhang, B. Recent advances in non-noble metal electrocatalysts for nitrate reduction. *Chem. Eng. J.* **2021**, *403*, No. 126269.
(22) Fan, K.; Xie, W.; Li, J.; Sun, Y.; Xu, P.; Tang, Y.; Li, Z.; Shao, M. Active hydrogen boosts electrochemical nitrate reduction to ammonia. *Nat. Commun.* **2022**, *13*, 7958.
(23) Li, H.; Yan, C.; Guo, H.; Shin, K.; Humphrey, S. M.; Werth, C. J.; Henkelman, G. Cu_xIr_{1-x} nanoalloy catalysts achieve near 100% selectivity for aqueous nitrite reduction to NH_3. *ACS Catal.* **2020**, *10*, 7915−7921.
(24) Lim, J.; Liu, C. Y.; Park, J.; Liu, Y. H.; Senftle, T. P.; Lee, S. W.; Hatzell, M. C. Structure sensitivity of Pd facets for enhanced electrochemical nitrate reduction to ammonia. *ACS Catal.* **2021**, *11*, 7568−7577.
(25) Gao, W.; Xie, K.; Xie, J.; Wang, X.; Zhang, H.; Chen, S.; Wang, H.; Li, Z.; Li, C. Alloying of Cu with Ru enabling the relay catalysis for reduction of nitrate to ammonia. *Adv. Mater.* **2023**, *35*, No. 2202952.
(26) Liu, H.; Park, J.; Chen, Y.; Qiu, Y.; Cheng, Y.; Srivastava, K.; Gu, S.; Shanks, B. H.; Roling, L. T.; Li, W. Electrocatalytic nitrate reduction on oxide-derived silver with tunable selectivity to nitrite and ammonia. *ACS Catal.* **2021**, *11*, 8431−8442.
(27) Yin, H.; Peng, Y.; Li, J. Electrocatalytic reduction of nitrate to ammonia via a Au/Cu single atom alloy catalyst. *Environ. Sci. Technol.* **2023**, *57*, 3134−3144.
(28) Yang, H. Y.; He, K. Y.; Ai, X.; Liu, X.; Yang, Y.; Yin, S. B.; Jin, P. J.; Chen, Y. Pyridine functionalized silver nanosheets for nitrate electroreduction. *J. Mater. Chem. A* **2023**, *11*, 16068−16073.
(29) Liu, J. X.; Richards, D.; Singh, N.; Goldsmith, B. R. Activity and selectivity trends in electrocatalytic nitrate reduction on transition metals. *ACS Catal.* **2019**, *9*, 7052−7064.
(30) Cheng, R.; Min, Y.; Li, H.; Fu, C. Electronic structure regulation in the design of low-cost efficient electrocatalysts: From theory to applications. *Nano Energy* **2023**, *115*, No. 108718.
(31) Abeyweera, S. C.; Yu, J.; Perdew, J. P.; Yan, Q.; Sun, Y. Hierarchically 3D porous Ag nanostructures derived from silver benzenethiolate nanoboxes: Enabling CO_2 reduction with a near-unity selectivity and mass-specific current density over 500 A/g. *Nano Lett.* **2020**, *20*, 2806−2811.
(32) Huang, Y.; Tang, C.; Li, Q.; Gong, J. Computational studies for boosting nitrate electroreduction activity of Fe-N_4-C Single-Atom catalyst via axial fifth ligand. *Appl. Surf. Sci.* **2023**, *616*, No. 156440.
(33) Gao, D.; Zhang, Y.; Zhou, Z.; Cai, F.; Zhao, X.; Huang, W.; Li, Y.; Zhu, J.; Liu, P.; Yang, F.; Wang, G.; Bao, X. Enhancing CO_2 electroreduction with the metal-oxide interface. *J. Am. Chem. Soc.* **2017**, *139*, 5652−5655.
(34) Battocchio, C.; Porcaro, F.; Mukherjee, S.; Magnano, E.; Nappini, S.; Fratoddi, I.; Quintiliani, M.; Russo, M. V.; Polzonetti, G. Gold nanoparticles stabilized with aromatic thiols: Interaction at the molecule-metal interface and ligand arrangement in the molecular shell investigated by SR-XPS and NEXAFS. *J. Phys. Chem. C* **2014**, *118*, 8159−8168.
(35) Li, L.; Tang, C.; Cui, X.; Zheng, Y.; Wang, X.; Xu, H.; Zhang, S.; Shao, T.; Davey, K.; Qiao, S. Z. Efficient nitrogen fixation to ammonia through integration of plasma oxidation with electrocatalytic reduction. *Angew. Chem., Int. Ed.* **2021**, *133*, 14250−14256.
(36) Song, Z.; Liu, Y.; Zhong, Y.; Guo, Q.; Zeng, J.; Geng, Z. Efficient electroreduction of nitrate into ammonia at ultralow concentrations via an enrichment effect. *Adv. Mater.* **2022**, *34*, No. 2204306.
(37) Song, Z.; Qin, L.; Liu, Y.; Zhong, Y.; Guo, Q.; Geng, Z.; Zeng, J. Efficient electroreduction of nitrate to ammonia with CuPd nanoalloy catalysts. *ChemSusChem* **2023**, *16*, No. e202300202.
(38) Yoon, Y.; Yan, B.; Surendranath, Y. Suppressing Ion Transfer Enables Versatile Measurements of Electrochemical Surface Area for Intrinsic Activity Comparisons. *J. Am. Chem. Soc.* **2018**, *140*, 2397−2400.
(39) Niu, Z.; Fan, S.; Li, X.; Wang, P.; Liu, Z.; Wang, J.; Bai, C.; Zhang, D. Bifunctional copper-cobalt spinel electrocatalysts for efficient tandem-like nitrate reduction to ammonia. *Chem. Eng. J.* **2022**, *450*, No. 138343.
(40) Costa, G. F.; Pinto, M. R.; Messias, I.; Junior, J.; Singh, N.; Nagao, R. Tracking copper oxidation state during nitrate electrochemical reduction reaction. *Meet. Abstr.* **2023**, *MA2023-01*, 2300.
(41) De, D.; Englehardt, J. D.; Kalu, E. E. Electroreduction of nitrate and nitrite ion on a platinum-group-metal catalyst-modified carbon fiber electrode chronoamperometry and mechanism studies. *J. Electrochem. Soc.* **2000**, *147*, 4573.

(42) Albery, W. J. Electrode kinetics. *Philos. Trans. R. Soc. London A* **1981**, *302*, 221−235.

https://doi.org/10.1021/prechem.3c00107
Precis. Chem. 2024, 2, 112−119